

# Temperature Effect on Corrosion Behavior of 304LN Stainless Steel and Carbon Steel Rebars in Chloride Contaminated Concrete Pore Solution Using Electrochemical Method

Bo Dong<sup>1</sup>, Xiao-Dong Wen<sup>2,\*</sup>, Lei Feng<sup>2</sup>

<sup>1</sup>Lancang-Mekong International Vocational Institute & School of Vocational and Technical Education, Yunnan University of Nationalities, Kunming 650504, Yunnan, China

<sup>2</sup>Zhejiang Engineering Technology Research Center of Civil Engineering Industrialized Construction, Ningbo University of Technology, Ningbo 315211, Zhejiang, China

\*E-mail: [wenxiaodong@nbut.edu.cn](mailto:wenxiaodong@nbut.edu.cn)

*Received:* 2 May 2020 / *Accepted:* 13 June 2020 / *Published:* 30 September 2020

---

Corrosion of steel rebars in alkaline environments can be exacerbated in hot weather conditions, which has a direct impact on the durability of reinforced concrete structures. Here, the corrosion resistance of 304LN stainless steel and carbon steel rebars were studied using the electrochemical impedance spectroscopy and potentiodynamic polarization techniques in chloride contaminated concrete pore solution at various temperatures. Corrosion rate of all samples had increased with increasing exposure temperatures from 25 °C to 55 °C. Polarization data revealed enhanced corrosion resistance of stainless steel rebar under hot alkaline environments compared to carbon steel rebar which can be attributed to the formation of chemically stable, thin and passive oxide layer caused by chromium into the stainless steel structures. The electrochemical results indicate that 304LN stainless steels reveal a higher impedance with a higher durability, lower corrosion current density, and higher corrosion resistance than carbon steel.

---

**Keywords:** Corrosion resistance; Concrete pore solution; Stainless steel rebar; Temperature effect; Electrochemical techniques

## 1. INTRODUCTION

Reinforced concrete structures have been widely used in construction because of their service lifetime, reliability and durability [1-3]. However, corrosion of steel reinforcement by aggressive environments such as carbon dioxide and chlorides, deterioration of mechanical performance, and cracking of concrete coatings can lead to premature destruction of concrete structures [4, 5]. The common materials used for reinforcement are carbon steel and stainless steel rebars [6, 7]. When steel

rebars are embedded in concrete, they become passive because of the formation of thin and protective oxide film [8, 9]. This film is very stable in an alkaline media. The stability of the passive layer is highly dependent on the film dissolution and film growth. In this case, temperature seems to be a related parameter in the passive film stability. Several methods have been suggested to consider for this effect [10, 11]. The critical pitting temperature experiments have been widely used to study the corrosion resistance of stainless steel rebar [12, 13].

The so-called cyclic thermometry method has also been used to evaluate the critical passivation temperature of Al in nitric acid media [14]. Furthermore, temperature transients have been employed as helpful thermal technique for passivity investigations of Ni-based alloys [15, 16]. Regarding the behavior of metal reinforcements in concrete, there are some reports on the temperature effect on corrosion rates in isothermal conditions [17, 18]. However, these researches don't report analytical findings and their more correlation to electrochemical results attained at different temperature. To date, all studies have been limited to phenomenological explanations of the several environmental effects and attempt has been made to deep evaluate the type of rebar with its electrochemical behavior in temperature changes. Therefore, the current study focused on the investigation of corrosion potentials caused by temperature variations, introducing new approach about the temperature role in the electrochemical corrosion of carbon steel and stainless steel rebars.

## 2. MATERIALS AND METHOD

Steel samples, 30 cm long and 1.5 cm diameter, were used for corrosion investigations. The surfaces of all samples were cleaned with acetone, washed and dried in distilled water and in air, respectively. The ends of the steel samples were coated by an epoxy resin. Two types of rebars, namely 304LN stainless steel (SS) and carbon steel (CS), were studied. The chemical composition of steel samples applied in this work is shown in Table 1.

**Table 1.** Chemical compositions of steel rebars (wt%)

Steels	Fe	Ni	C	Mn	Si	P	S	Cr
304LN stainless steel	Remainder	9.5	0.03	1.55	0.50	0.03	0.025	19.5
Carbon steel	Remainder	0.029	0.27	0.68	0.22	0.026	0.025	0.016

**Table 2.** Concentration of SCPS admixtures

SCPS admixtures	Concentration
Ca(OH) <sub>2</sub>	0.3 mol/dm <sup>3</sup>
KOH	0.5 mol/dm <sup>3</sup>
NaOH	0.2 mol/dm <sup>3</sup>

To prepared simulated concrete pore solution (SCPS) environment, a mixture of  $\text{Ca}(\text{OH})_2$ ,  $\text{KOH}$  and  $\text{NaOH}$  with 13.5 pH was used. Table 2 indicates the concentration of SCPS admixtures.

The electrochemical experiments were done using a three-electrode electrochemical cell setup with steel samples, a graphite rod and a saturated calomel electrodes as working electrode, counter and saturated calomel electrodes, respectively. The samples were immersed into the SCPS including 3wt%  $\text{CaCl}_2$  as chloride ion source. Four exposure temperatures, 25, 35, 45 and 55 °C, were selected as seasonal variation of temperatures in hot-SCPS environments.

Electrochemical impedance spectroscopy (EIS) measurements were done in the frequency range from 0.1 MHz to 0.1 mHz at the open circuit potential with  $\pm 10$  mV AC perturbation. The potentiodynamic polarization analysis was carried out at scanning rate of 1 mV/s. The morphologies of steel samples were studied by a Zeiss Sigma scanning electron microscope (SEM).

### 3. RESULTS AND DISCUSSION

Figure 1 shows the changes of open circuit potential exposed to SCPS environment with different exposure time for 304LN SS rebar at four tested temperatures. At 25 °C temperature, the corrosion potential of 304LN steel rebar was maintained stable during the analysis process. However, with increasing immersion time the potential of the samples shifted toward the noble direction at 35, 45 and 55 °C.

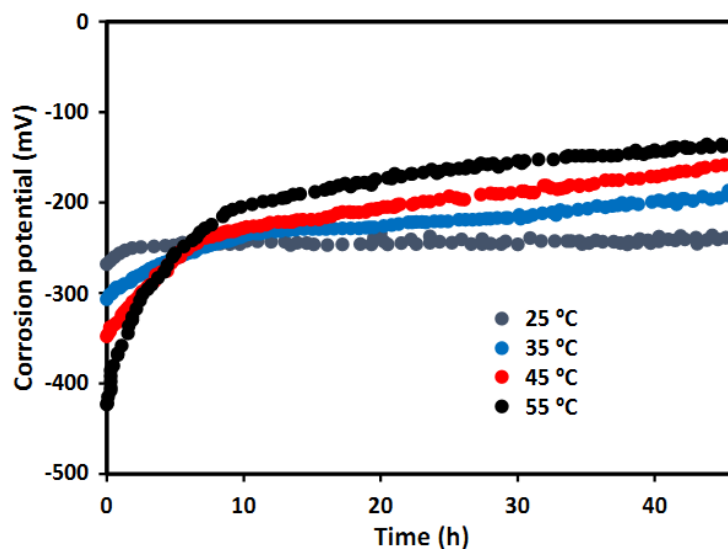


**Figure 1.** Open circuit potential for 304LN SS rebar exposed to SCPS environment at four tested temperatures

At the beginning of exposure time, a greater negative potential was recorded at temperature of 55 °C which may be associated to lower oxygen content in SCPS environment. Indeed, Figure 1 indicates that corrosion potential of 304LN SS rebar cannot be detected only by the solution chemistry. Thus, it appears that additional processes in the interface of solution-metal are significantly involved in

explaining the observed changes. In alkaline environment, passive layers of Fe-based alloys show redox-behavior of magnetite [19, 20]. The magnetite oxidation increases the surface resistance and therefore moves the corrosion potential toward a more noble direction. This process is commonly referred to as ageing of the passive layer [21]. Structural changes caused by temperature in the passive film have main influences on a long-term corrosion behavior of 304LN SS rebar due to the reduction in film thickening and barrier properties.

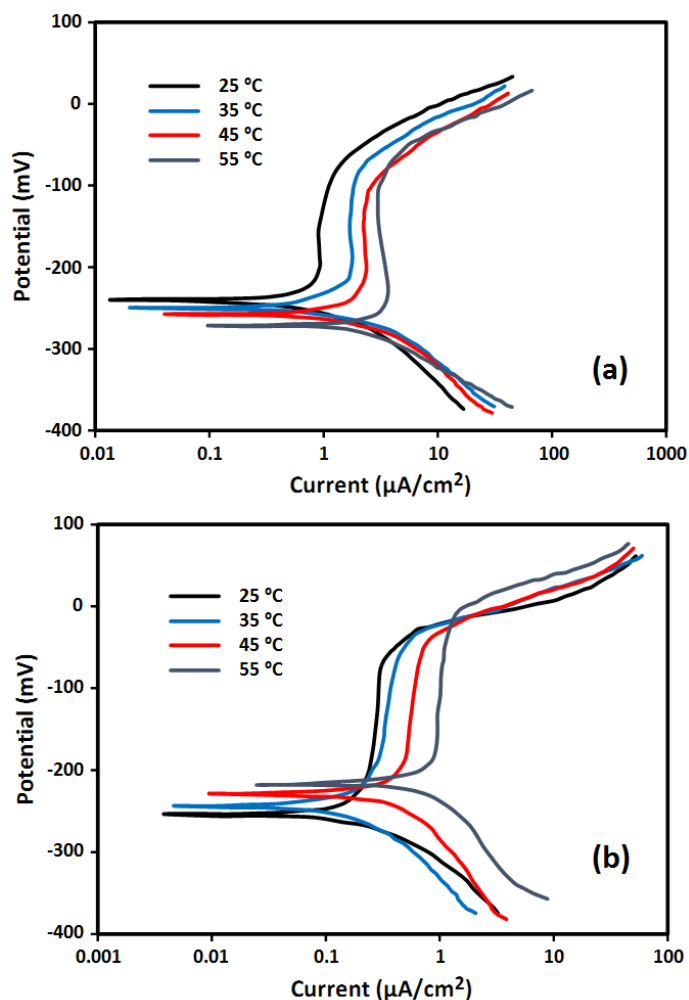
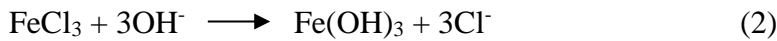


**Figure 2.** Polarization curves of (a) carbon steel and (b) 304LN SS rebar exposed to SCPS environment containing 3 wt% chloride ions at various temperatures after 12 h immersion time at scanning rate of 1 mV/s

Figure 2a shows the polarization curves of carbon steel rebar exposed to SCPS environment containing 3 wt% chloride ions at various temperatures. The polarization curves for the samples immersed in 55 °C shifted to the anodic direction revealing an enhancement of the corrosion rate compared to other samples exposed to lower temperatures. It can be attributed to the reaction rate of chloride with Fe ions which can be significantly affected by the reaction kinetics with increasing temperature, as explained in Eqs. (1) and (2).





Corrosion product with the formation of  $\text{Fe}(\text{OH})_2$  and  $\text{Fe}_2\text{O}_3$  as the intermediate product were created, as indicated in Eqs (3) and (4).



The electrochemical parameters can be valued by a curve-fitting technique in the weak-polarization behavior of the samples [22]. The parameter values are listed in Table 2.

**Table 2.** Fitting electrochemical parameters of the samples obtained from polarization plots.

Sample	Temperature	Corrosion current density ( $\mu\text{Acm}^{-2}$ )	Corrosion potential (mV)
304LN SS	25 °C	0.25	-261
	35 °C	0.31	-242
	45 °C	0.62	-228
	55 °C	0.91	-217
Carbon steel	25 °C	0.96	-238
	35 °C	2.52	-252
	45 °C	3.44	-260
	55 °C	6.74	-276

Table 3 shows comparison of corrosion behavior of various steel rebars reported in previous studies. The results indicate that the corrosion behavior of 304LN SS were comparable with other steel rebars obtained from the literature.

**Table 3.** Comparison of corrosion behavior of various steel rebars reported in previous studies

Rebar	Environment	Temperature	Corrosion potential (mV)	Corrosion current density ( $\mu\text{Acm}^{-2}$ )	Ref.
HRB400 steel	SCPS	25 °C	-247	0.13	[23]
AISI 316 LN SS	SCPS	25 °C	-354	2.2	[6]
Mild steel	3.5 wt.% NaCl	40 °C	-400	16.45	[24]
316 LN SS	SCPS	25 °C	-251	0.1	[25]
304LN SS	SCPS	25 °C	-261	0.25	This work

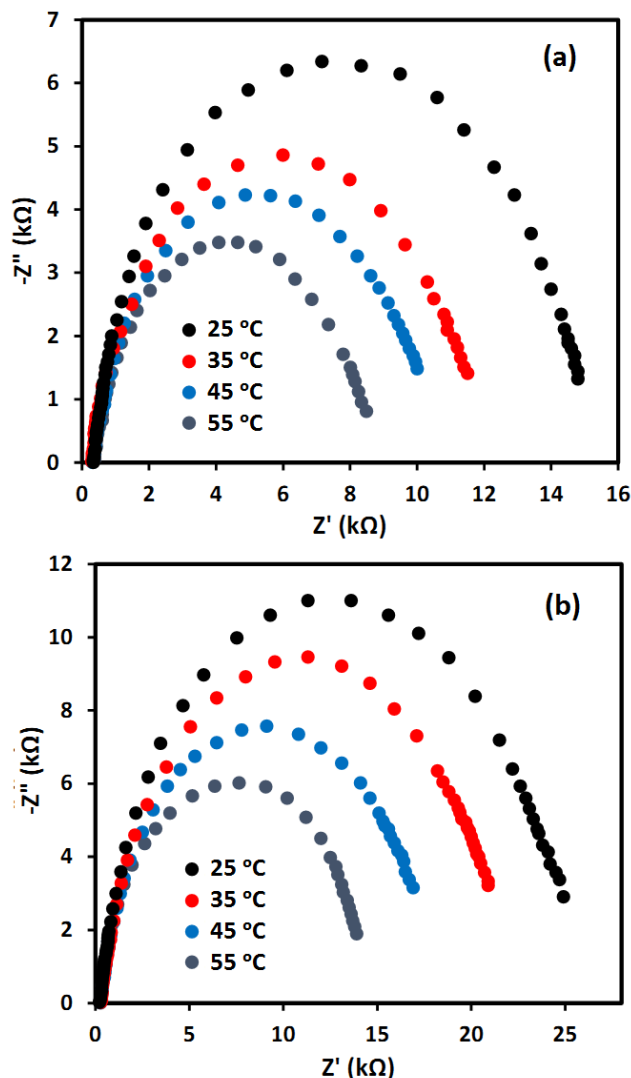


**Figure 3.** EIS diagrams of (a) carbon steel and (b) 304LN SS rebars immersed in SCPS containing 3 wt% chloride ions at different temperatures in the frequency range from 0.1 MHz to 0.1 mHz

As shown in Table 2, 304LN SS bars at a corrosion potential of  $-280\text{mV}$  at  $25\text{ }^{\circ}\text{C}$  shifted to  $-200\text{mV}$  at  $55\text{ }^{\circ}\text{C}$  exposure temperature. Higher noble potentials obtained in the 304LN SS rebar compared to carbon steel rebar indicated more corrosion-resistant in 304LN SS rebar. It can be associated to the creation of chromium-oxide protective layer on the 304LN SS surface [26, 27]. However, a decrease in iron levels can also be a sign of localized corrosion of the pitting. Furthermore, the corrosion current densities of 304LN SS rebar showed lower values than the carbon steel rebar indicating more corrosion protective in 304LN SS samples.

Commonly, an increase in the SCPS temperature had a direct effect on corrosion current density of both tested rebars, as shown in Table 2. The  $I_{\text{corr}}$  of carbon steel samples were gradually increased by the increase of the SCPS temperature. Rising temperatures accelerate the corrosion process due to further dissolution of metals [28]. There was an almost slight increase in  $I_{\text{corr}}$  for 304LN SS rebar with increasing temperature which can be related to the presence of noble metal such as Cr in its composition.

EIS analysis were performed in order to investigate the electrochemical behavior of carbon steel and 304LN SS rebars in SCPS media after 12 h immersion time. Previous reports had studied this subject,

however, there is still disagreement about the EIS response of steel rebars in SCPS solution at different environment temperatures.

Figures 3 shows the Nyquist diagrams of the 304LN SS and carbon steel samples immersed in SCPS containing 3 wt% chloride ions at different temperatures. Nyquist plots typically show a capacitive loop that its diameter decreases as the temperature increases which can be associated to the more dissolution of steels. The EIS plots shows the resistance between the electrolyte solution and the working electrode for both rebars at the high-frequency. Furthermore, at the low-frequency, it can be related to the charge-transfer resistance into the corrosion process [29].

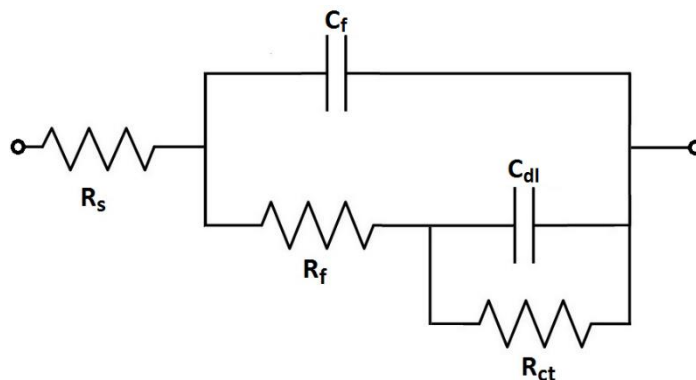


**Figure 4.** The equivalent circuit model

Figure 3 exhibits an equivalent circuit model with two time constants that proposed to simulate the EIS process of carbon steel and 304LN SS rebars in this study.

At higher frequencies,  $R_f$  and  $C_f$  show a resistance because of the ionic paths by the oxide film and capacitive behavior of formed passive layer, respectively. At the second time constant,  $R_{ct}$  and  $C_{dl}$  reveals the charge-transfer resistance and the capacitive behavior in the interfaces. The best fitting parameters based on the circuit depicted in figure 4 are summarized in Table 4. As shown, the  $R_{ct}$  values of carbon steel rebar are significantly decreased from 15.9 kΩ to 8.8 kΩ, as the temperature increases in the SCPS solution which show that the temperature had enhanced the corrosion behavior of the steel.

**Table 4.** EIS parameters derived from the fitting equivalent circuit

Rebar	Temperature	$R_s$ ( $\Omega \text{ cm}^2$ )	$R_f$ ( $\text{k}\Omega \text{ cm}^2$ )	$C_f$ ( $\mu\text{F cm}^{-2}$ )	$R_{ct}$ ( $\text{k}\Omega \text{ cm}^2$ )	$C_{dl}$ ( $\mu\text{F cm}^{-2}$ )
Carbon steel	25 °C	39.6	9.7	67.2	15.9	98.8
	35 °C	42.8	7.5	78.6	12.3	112.5
	45 °C	32.5	6.4	92.3	10.9	132.7
	55 °C	36.7	5.1	101.5	8.8	146.5
304LN SS	25 °C	71.2	17.9	18.7	27.4	32.6
	35 °C	85.6	13.8	31.2	22.3	59.7
	45 °C	74.8	10.4	58.6	18.1	86.2
	55 °C	69.3	8.9	72.4	14.2	102.7

Furthermore, Table 4 exhibits that  $R_f$  gradually reduced by increasing the temperature for both rebars which indicates that porous products and non-protective corrosion had increased on the steel surface. These findings are consistent with the best-fit results for  $C_{dl}$  which were gradually increased at 55 °C in the SCPS solution, indicating that corrosion can happen on the steel surface. Furthermore,  $R_{ct}$  of the 304LN SS samples were larger than that of carbon steel samples which indicate superior corrosion resistance of 304LN SS rebars in SCPS media. It can be attributed to the presence of noble metal such as Cr in 304LN SS composition. 304LN SS rebars are produced by further addition of chromium element which cause the formation of chemically stable, thin and passive oxide layer [30].

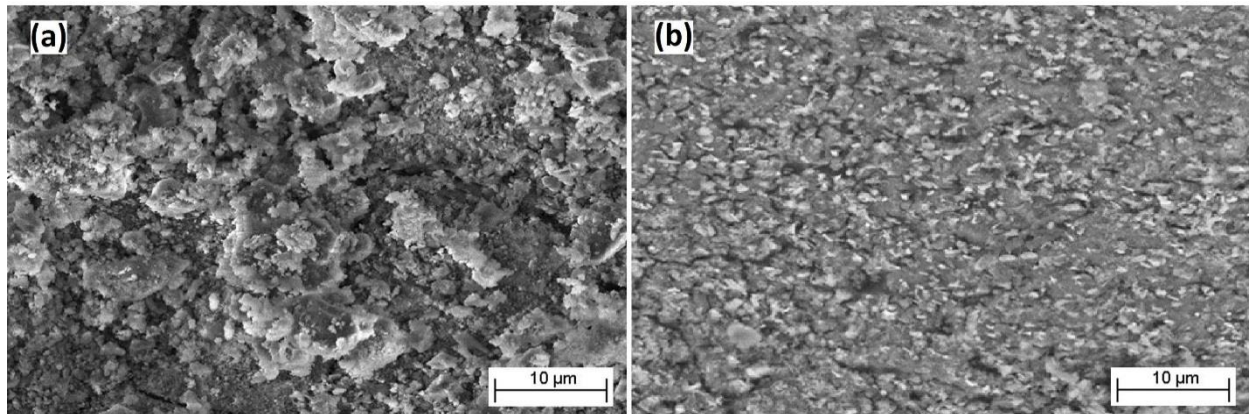


**Figure 5.** FESEM images of (a) carbon steel and (b) 304LN SS rebars exposed to the SCPS environment containing 3 wt% chloride ions at 55 °C temperature after 48 h immersion time

Figure 5 shows the FESEM images of carbon steel and 304LN SS rebars exposed to the SCPS environment containing 3 wt% chloride ions at 55 °C temperature after 48 h immersion time. Corrosion pitting on the carbon steel surface was more intense than that of 304LN SS rebar, indicating that the 304LN SS samples showed a good corrosion resistance.

#### 4. CONCLUSIONS

The corrosion resistance of 304LN SS and carbon steel rebars were studied using the EIS and potentiodynamic polarization techniques in chloride contaminated SCPS at various temperatures. Corrosion rate of all samples had increased with the increase of exposure temperatures from 25 °C to 55 °C. Polarization data revealed enhanced corrosion resistance of 304LN SS rebar under hot alkaline environments compared to carbon steel rebar which can be attributed to the formation of chemically stable, thin and passive oxide layer caused by chromium on the 304LN SS structures. The electrochemical results indicate that 304LN SS rebars reveal a higher impedance with a higher durability, lower corrosion current density, and higher corrosion resistance than carbon steel.

#### ACKNOWLEDGEMENT

This work was sponsored in part by National Natural Science Foundation of China (51569035).

**References**

1. M. Akiyama, D.M. Frangopol and K. Takenaka, *Structure and Infrastructure Engineering*, 13 (2017) 468.
2. H. Karimi-Maleh and O.A. Arotiba, *Journal of colloid and interface science*, 560 (2020) 208.
3. S. Kakooei, H.M. Akil, M. Jamshidi and J. Rouhi, *Construction and Building Materials*, 27 (2012) 73.
4. A.M. Aguirre-Guerrero, R.A. Robayo-Salazar and R.M. de Gutiérrez, *Applied Clay Science*, 135 (2017) 437.
5. Y. Shen, Y. Dong, H. Li, X. Chang, D. Wang, Q. Li and Y. Yin, *International Journal of Electrochemical Science*, 13 (2018) 6310.
6. U. Martin, J. Ress, J. Bosch and D. Bastidas, *Electrochimica Acta*, 335 (2020) 135565.
7. F. Tahernejad-Javazmi, M. Shabani-Nooshabadi and H. Karimi-Maleh, *Composites Part B: Engineering*, 172 (2019) 666.
8. R. Chen, J. Hu, Y. Ma, W. Guo, H. Huang, J. Wei, S. Yin and Q. Yu, *Corrosion Science*, 165 (2020) 108393.
9. J. Rouhi, C.R. Ooi, S. Mahmud and M.R. Mahmood, *Electronic Materials Letters*, 11 (2015) 957.
10. B. Li, Y. Huan and W. Zhang, *International Journal of Electrochemical Science*, 12 (2017) 10402.
11. A. Khodadadi, E. Faghieh-Mirzaei, H. Karimi-Maleh, A. Abbaspourrad, S. Agarwal and V.K. Gupta, *Sensors and actuators b: chemical*, 284 (2019) 568.
12. R. Tavassolian, M.H. Moayed and I. Taji, *Journal of The Electrochemical Society*, 166 (2019) C101.
13. Z. Shamsadin-Azad, M.A. Taher, S. Cheraghi and H. Karimi-Maleh, *Journal of Food Measurement and Characterization*, 13 (2019) 1781.
14. X. Wu, Y. Yang, Y. Sun, Y. Liu, J. Li and Y. Jiang, *Corrosion Science*, 149 (2019) 29.
15. E. Sadeghimeresht, N. Markocsan, M. Huhtakangas and S. Joshi, *Surface and Coatings Technology*, 316 (2017) 10.
16. H. Karimi-Maleh, C.T. Fakude, N. Mabuba, G.M. Peleyeju and O.A. Arotiba, *Journal of colloid and interface science*, 554 (2019) 603.
17. M. Stefanoni, U. Angst and B. Elsener, *Cement and Concrete Research*, 103 (2018) 35.
18. N. Yermak, P. Pliya, A.-L. Beaucour, A. Simon and A. Noumowé, *Construction and Building Materials*, 132 (2017) 240.
19. M. Sánchez, J. Gregori and C. Alonso, *Electrochim. acta*, 52 (2007) 7634.
20. S. Kakooei, H.M. Akil, A. Dolati and J. Rouhi, *Construction and Building Materials*, 35 (2012) 564.
21. N. Kauss, A. Heyn, T. Halle and P. Rosemann, *Electrochimica Acta*, 317 (2019) 17.
22. J.W. Wu, D. Bai, A. Baker, Z.H. Li and X.B. Liu, *Materials and corrosion*, 66 (2015) 143.
23. Z. Ai, J. Jiang, W. Sun, D. Song, H. Ma, J. Zhang and D. Wang, *Applied Surface Science*, 389 (2016) 1126.
24. M. Fouladi and A. Amadeh, *Electrochimica Acta*, 106 (2013) 1.
25. A.A. Adewumi, M. Maslehuddin, S.U. Al-Dulaijan and M. Shameem, *European Journal of Environmental and Civil Engineering*, (2018) 1.
26. M. Rabani, M. Zandrahimi and H. Ebrahimifar, *International Journal of Iron & Steel Society of Iran*, 16 (2019) 41.
27. J. Rouhi, S. Mahmud, S. Hutagalung and S. Kakooei, *Micro & Nano Letters*, 7 (2012) 325.
28. H. Liu, F. Cao, G.-L. Song, D. Zheng, Z. Shi, M.S. Dargusch and A. Atrens, *Journal of Materials Science & Technology*, 35 (2019) 2003.

29. J. Rouhi, S. Kakooei, M.C. Ismail, R. Karimzadeh and M.R. Mahmood, *International Journal of Electrochemical Science*, 12 (2017) 9933.
30. G. Karafyllias, A. Galloway and E. Humphries, *Wear*, 420 (2019) 79.

© 2020 The Authors. Published by ESG ([www.electrochemsci.org](http://www.electrochemsci.org)). This article is an open access article distributed under the terms and conditions of the Creative Commons Attribution license (<http://creativecommons.org/licenses/by/4.0/>).